The EMBO Journal Vol.17 No.3 pp.774–785, 1998

Targeted disruption of the MYC antagonist MAD1 inhibits cell cycle exit during granulocyte differentiation

Kevin P.Foley, Grant A.McArthur, Christophe Quéva, Peter J.Hurlin, Philippe Soriano and Robert N.Eisenman[1]

Division of Basic Sciences, Fred Hutchinson Cancer Research Center, 1100 Fairview Avenue North–Mailstop A2-025, P.O. Box 19024, Seattle, WA 98109-1024, USA

[1]Corresponding author
e-mail: eisenman@fred.fhcrc.org

K.P.Foley and G.A.McArthur contributed equally to this work

The switch from transcriptionally activating MYC–MAX to transcriptionally repressing MAD1–MAX protein heterodimers has been correlated with the initiation of terminal differentiation in many cell types. To investigate the function of MAD1–MAX dimers during differentiation, we disrupted the *Mad1* gene by homologous recombination in mice. Analysis of hematopoietic differentiation in homozygous mutant animals revealed that cell cycle exit of granulocytic precursors was inhibited following the colony-forming cell stage, resulting in increased proliferation and delayed terminal differentiation of low proliferative potential cluster-forming cells. Surprisingly, the numbers of terminally differentiated bone marrow and peripheral blood granulocytes were essentially unchanged in *Mad1* null mice. This imbalance between the frequencies of precursor and mature granulocytes was correlated with a compensatory decrease in granulocytic cluster-forming cell survival under apoptosis-inducing conditions. In addition, recovery of the peripheral granulocyte compartment following bone marrow ablation was significantly enhanced in *Mad1* knockout mice. Two *Mad1*-related genes, *Mxi1* and *Mad3*, were found to be expressed ectopically in adult spleen, indicating that functional redundancy and cross-regulation between MAD family members may allow for apparently normal differentiation in the absence of MAD1. These findings demonstrate that MAD1 regulates cell cycle withdrawal during a late stage of granulocyte differentiation, and suggest that the relative levels of MYC versus MAD1 mediate a balance between cell proliferation and terminal differentiation.

Keywords: cell cycle exit/granulocyte/MAD1/MYC/terminal differentiation

Introduction

Appropriate regulation of the opposing processes of cell proliferation and terminal differentiation is a critical aspect of normal development and homeostasis (Raff, 1996), and is frequently disrupted during tumorigenesis (Sawyers *et al.*, 1991). Considerable progress has been made in recent years towards understanding the signaling pathways through which environmental stimuli, such as growth factors or cell–cell interactions, regulate the commitment of multipotential precursors to specific cell lineages and their subsequent proliferation (Morrison *et al.*, 1997). However, the mechanisms by which these lineage-committed cells cease to divide at the appropriate time and take on a terminally differentiated phenotype remain poorly understood.

The c-, L- and N-MYC oncoproteins (collectively termed MYC) are thought to be key regulators of proliferation in most cell types (Marcu *et al.*, 1992; Henriksson and Lüscher, 1996). MYC activates transcription by binding to CACGTG-response elements as a heterodimer with MAX (Blackwood and Eisenman, 1991; Prendergast *et al.*, 1991; Amati *et al.*, 1992; Kretzner *et al.*, 1992), and several candidate MYC–MAX target genes have been identified (Grandori and Eisenman, 1997). Since MAX is widely and constitutively expressed, the formation of MYC–MAX dimers is dependent upon the rate of MYC synthesis (Blackwood *et al.*, 1992). MYC expression is induced rapidly in response to mitogenic stimulation and is down-regulated as cells exit the cell cycle and become quiescent (Kelly *et al.*, 1982). Several lines of evidence suggest that MYC is required as a rate-limiting step during cell cycle entry and the G_1–S transition. For example, ectopic expression of MYC is sufficient to induce cell cycle re-entry of a serum-starved fibroblast cell line (Eilers *et al.*, 1991), although, in the absence of survival cytokines, MYC-induced proliferation also results in apoptotic cell death (Askew *et al.*, 1991; Evan *et al.*, 1992). In contrast, antisense oligonucleotides that block MYC expression inhibit cell cycle entry at the G_1–S transition (Heikkila *et al.*, 1987), and targeted inactivation of MYC in mice results in mid-gestational lethality due to the failure of cell proliferation during organogenesis (Morgenbesser and DePinho, 1994). Notably, MYC is down-regulated during differentiation (Westin *et al.*, 1982; Lachman and Skoultchi, 1984), and its ectopic expression can inhibit cell cycle withdrawal and terminal differentiation of many cell types (Coppola and Cole, 1986; Langdon *et al.*, 1986; Freytag, 1988).

Members of the MAD protein family (MAD1, MXI1, MAD3 and MAD4) compete with MYC for heterodimerization to MAX (Ayer and Eisenman, 1993; Ayer *et al.*, 1993; Zervos *et al.*, 1993; Hurlin *et al.*, 1995b). However, in contrast to MYC–MAX, MAD1–MAX dimers repress transcription of CACGTG-containing genes (Ayer *et al.*, 1993; Hurlin *et al.*, 1995b). Ectopic expression of MAD1 has been found to inhibit proliferation by promoting G_1 cell cycle arrest (Chen *et al.*, 1995; Roussel *et al.*, 1996), and can block transformation of rat embryo fibroblasts by *Myc* (Lahoz *et al.*, 1994; Cerni *et al.*, 1995; Koskinen *et al.*, 1995; Västrik *et al.*, 1995). Ectopically expressed

MAD1 can also over-ride the ability of MYC to inhibit terminal differentiation of murine erythroleukemia cells (Cultraro *et al.*, 1997). These activities of MADs depend upon formation of a ternary complex between MAD–MAX and mSIN3A or mSIN3B (Ayer *et al.*, 1995; Hurlin *et al.*, 1995b; Schreiber-Agus *et al.*, 1995), co-repressors that can in turn recruit histone deacetylases to target genes (Alland *et al.*, 1997; Hassig *et al.*, 1997; Heinzel *et al.*, 1997; Laherty *et al.*, 1997; Sommer *et al.*, 1997). Recently, a novel ubiquitously expressed MAX partner, MNT, has been identified that shares many of the attributes of MAD1 (Hurlin *et al.*, 1997; Meroni *et al.*, 1997).

Further insight into the possible *in vivo* functions of MAD1 and its relatives has come from studies of their expression patterns. Typically, the *Mad1* gene is expressed at low levels in proliferating cells and is up-regulated during terminal differentiation of most cell types (Chin *et al.*, 1995; Delgado *et al.*, 1995; Gandarillas and Watt, 1995; Hurlin *et al.*, 1995a,b; Västrik *et al.*, 1995; Lymboussaki *et al.*, 1996; Rao *et al.*, 1996; Cultraro *et al.*, 1997; Quéva *et al.*, 1998), often as an immediate early response to differentiation-inducing stimuli (Ayer and Eisenman, 1993; Larsson *et al.*, 1994). With the parallel down-regulation of MYC, this results in a switch from MYC–MAX to MAD1–MAX complexes as terminal differentiation proceeds (Ayer and Eisenman, 1993; Hurlin *et al.*, 1995a; Cultraro *et al.*, 1997). The different members of the *Mad* gene family are expressed in distinct, yet partially overlapping patterns (Hurlin *et al.*, 1995b; Quéva *et al.*, 1998). In developing mouse embryos, expression of the *Mad* family is first apparent with the onset of widespread differentiation during organogenesis while, in the adult, their expression is limited to tissues in which terminal differentiation is ongoing due to the presence of residual progenitor cells.

The ability of ectopic MAD1 to promote cell cycle arrest, along with the observed correlation between its expression and the commencement of terminal differentiation, has led us to propose that MAD1 negatively regulates proliferation-associated MYC target genes, thereby mediating cell cycle withdrawal and terminal differentiation. To date, however, a functional role for the MAD family during differentiation has yet to be demonstrated directly. To test this hypothesis, we have analyzed terminal differentiation in mice bearing homozygous *Mad1* null mutations.

Results

Targeted disruption of the murine Mad1 gene

To examine the *in vivo* function of MAD1, we generated targeted disruptions of the murine *Mad1* gene by homologous recombination in embryonic stem (ES) cells. Two different gene replacement vectors were designed, p*Mad1*^{tm1} (Figure 1A) and p*Mad1*^{tm2} (not shown), in which overlapping portions of the *Mad1* first exon and promoter region were deleted and replaced by the neomycin resistance (*neo*) gene. Following standard procedures, ES cells were electroporated with the targeting vectors, placed under positive/negative selection, and the surviving colonies screened for homologous recombination by PCR and Southern blotting (Figure 1A). Correct gene targeting occurred in ~18–32% of surviving *Mad1*^{tm1} and 94% of *Mad1*^{tm2} clones. Homologous recombination by both of these vectors was expected to result in the generation of null alleles due to deletion of the translation initiation codon, as well as the mSIN3 co-repressor interaction domain that is required for MAD1 function (Ayer *et al.*, 1993).

Three lines of knockout mice, representing one *Mad1*^{tm1} and two *Mad1*^{tm2} ES cell clones, were derived on the inbred 129/Sv genetic background. The progeny of matings between heterozygotes were analyzed by Southern blotting to identify wild-type (*Mad1*$^{+/+}$), heterozygous and homozygous (*Mad1*$^{-/-}$) mutant offspring (Figure 1B), which were found to be present at the expected Mendalian ratio (24:50:26, respectively; $n = 262$). *Mad1*$^{-/-}$ animals were viable, appeared outwardly normal and showed no obvious differences in size, behavior, reproductive ability, incidence of neoplasia or life spans when compared with *Mad1*$^{+/+}$ littermates. For the experiments described below, similar phenotypes were observed for each line, as well as for animals on the hybrid 129B6F2 and N_4-C57BL/6 genetic backgrounds.

To confirm that the *Mad1* gene was disrupted successfully, *Mad1* expression was examined by RT–PCR using primers specific for downstream exons which were not deleted by the gene targeting events. No *Mad1* expression was detected in any adult tissues from *Mad1*$^{-/-}$ mice (Figure 1C), demonstrating that null alleles had indeed been generated. The lack of *Mad1* expression was also confirmed by mRNA *in situ* hybridization analysis of embryonic and adult tissues, as described below (see Figure 7A and B).

Analysis of myeloid differentiation in Mad1 knockout mice

The hematopoietic system is particularly amenable for studying the switch from proliferation to terminal differentiation. Since MAD1 is induced as proliferating cells commit to terminal differentiation, we therefore proceeded carefully to examine hematopoiesis in these animals. Adult *Mad1*$^{-/-}$ and *Mad1*$^{+/+}$ littermates (8–11 weeks old) were analyzed by fluorescence-activated cell sorting (FACS) using antibodies to lineage-specific cell surface markers. We found a modest but statistically significant increase in the frequency of mature granulocytes in the bone marrow of *Mad1*$^{-/-}$ mice (Figure 2A and B, see Gran/Mac and Gran). Since homeostatic compensation can often ameliorate more severe underlying defects, we proceeded to investigate this observation further. *In vitro* bone marrow colony assays were performed in semi-solid media in the presence of concentrations of recombinant cytokines that were empirically determined to promote maximal cell proliferation and survival. The ability of bone marrow precursors to proliferate *in vitro* can be used to classify their stages of differentiation (Metcalf, 1984). Typically, immature lineage-committed colony-forming cells (CFCs) form groups of ~50 or more mostly terminally differentiated cells after 7 days of culture, whereas more mature cluster-forming cells (cluster-FCs) with very limited proliferative potential form smaller groups of 4–16 terminally differentiated cells after 2 days of culture, which then fail to proliferate further. To examine the frequencies of these two different stages of myeloid cell differentiation, bone marrow cultures were stimulated with granulocyte–macrophage colony-stimulating factor (GM-CSF) to promote

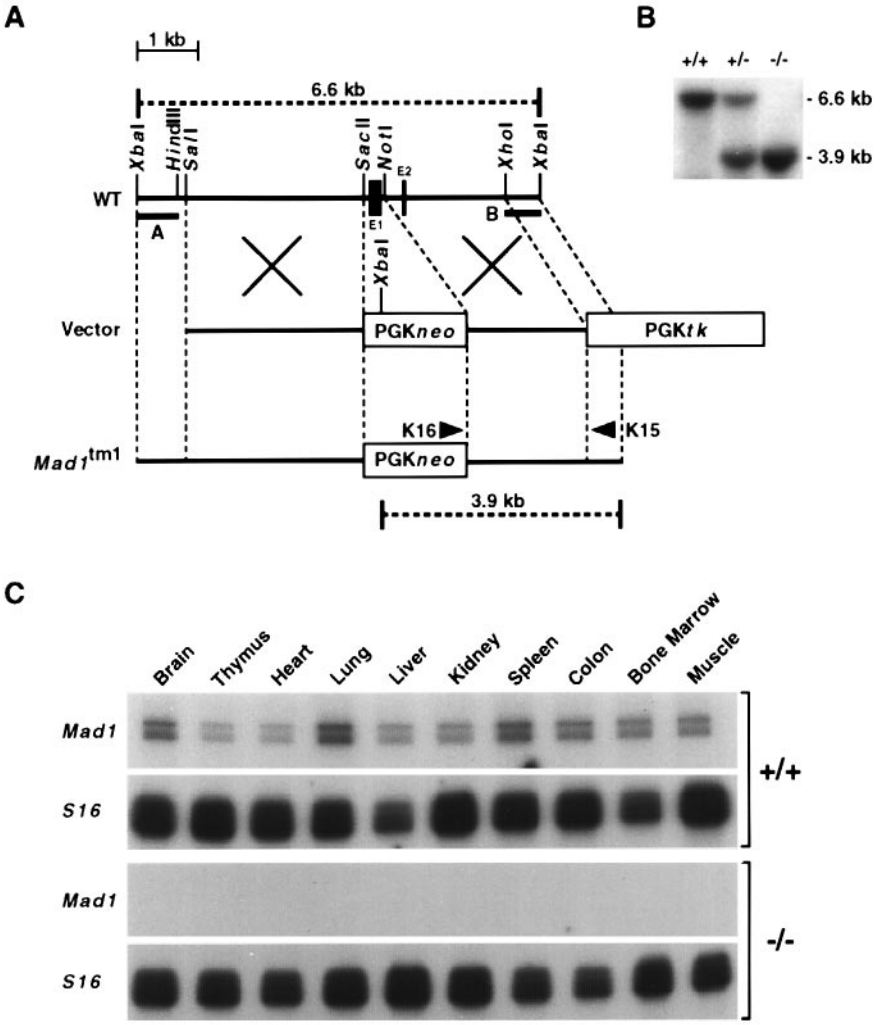

Fig. 1. Targeted disruption of the murine *Mad1* gene. (**A**) Partial restriction endonuclease map of the wild-type murine *Mad1* locus (WT), structure of the p*Mad1*^{tm1} targeting vector (Vector) and resulting homologous recombinant allele (*Mad1*^{tm1}) in which the *Mad1* promoter and first exon (containing the 5′ untranslated region and translational initiation codon) were deleted. E1 and E2 represent exons 1 and 2, respectively. *neo* and thymidine kinase (*tk*) genes under control of the mouse phosphoglycerate kinase 1 (PGK) promoter were used as positive and negative selectable markers, respectively. Crosses indicate expected areas of homologous recombination. PCR primers K15 and K16 (black arrowheads) were used to screen ES cell clones initially for correct homologous recombination. PCR-positive clones were analyzed with Southern probes A and B (horizontal bars) to confirm the recombinant 5′ and 3′ junctions, respectively. Also indicated are the expected sizes of *Xba*I bands (horizontal dashed lines) representing the wild-type and *Mad1*^{tm1} alleles detected by Southern hybridization with 3′ probe B. (**B**) Genomic Southern blot analysis using 3′ probe B of *Xba*I-digested tail DNA from progeny of a *Mad1*$^{+/-}$×*Mad1*$^{+/-}$ mating. (**C**) Denaturing polyacrylamide gel electrophoresis of radiolabeled RT–PCR reactions to detect *Mad1* expression in tissues from a *Mad1*^{tm1} homozygous mutant and wild-type littermate confirms that a null mutation was generated. Independent RT–PCR amplification of ribosomal protein S16 mRNA was used as a control for efficient cDNA synthesis. The doublet bands observed for both *Mad1* and S16 are probably due to independent migration of amplification product strands under denaturing conditions. Similar results were obtained for homozygous *Mad1*^{tm2} mice. Wild-type (+/+); heterozygote (+/–); homozygous mutant (–/–).

the survival and proliferation of both granulocytes and macrophages. We observed a 3-fold increase in the frequency of cluster-FCs in *Mad1*$^{-/-}$ cultures when compared with control cultures from *Mad1*$^{+/+}$ littermates (Figure 2A). Analysis of fixed cultures indicated that this increase represented predominantly granulocytic rather than macrophage clusters. Consistent with this, an increased frequency of granulocytic cluster-FCs was also observed when *Mad1*$^{-/-}$ bone marrow was stimulated with granulocyte colony-stimulating factor (G-CSF) (Figure 2B), which promotes the survival and proliferation of granulocytes but not macrophages. The frequency of granulocytic cluster-FCs in *Mad1*$^{+/-}$ heterozygotes was found to be intermediate between those of *Mad1*$^{+/+}$ and *Mad1*$^{-/-}$ mice (data not shown).

Importantly, no significant differences were found in the frequency of more immature granulocytic CFCs stimulated with either GM- or G-CSF (Figure 2A and B), suggesting a requirement for MAD1 only during the latter stages of granulocyte differentiation. This observation is consistent with the expression pattern of MAD1 protein in the murine granulocytic precursor cell line, MPRO, which can be induced to terminally differentiate by a retinoic acid receptor (RXR) agonist (Tsai and Collins, 1993; S.Collins, personal communication). Following treatment with the agonist, MAD1 expression was up-regulated in proliferating MPRO cells concomitant with the onset of cell cycle withdrawal, and reached a maximum in post-mitotic cells that exhibited a mature granulocyte morphology and expressed high levels of the Gr-1 differentiation marker

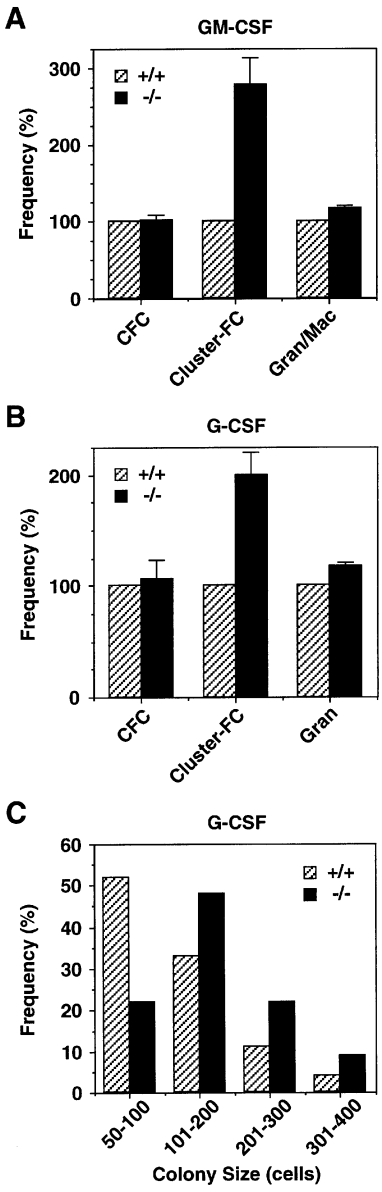

Fig. 2. Altered myelopoiesis in *Mad1*$^{-/-}$ mice. (A and B) *In vitro* hematopoietic colony formation from *Mad1*$^{-/-}$ (n = 7) bone marrow relative to *Mad1*$^{+/+}$ (n = 6) littermates. Immature committed CFCs and mature limited proliferative potential cluster-FCs were assayed in cultures of 25 000 bone marrow cells following stimulation with 1000 U/ml GM-CSF (**A**) or 1000 U/ml G-CSF (**B**). Cluster-FC frequencies were calculated by subtracting the number of colonies on day 7 from the number of clusters on day 2. Mature bone marrow granulocyte and macrophage cell numbers were determined by FACS with anti-Mac1 and anti-Gr-1 (Mac1/CD11b is expressed on both granulocytes and macrophages in 129/Sv mice). GM-CSF- and G-CSF-responsive cluster-FCs were significantly more abundant in *Mad1*$^{-/-}$ mice (cluster-FCs and mature cells, $P<0.01$). (**C**) Colonies (>50 cells by day 7 of culture) derived from G-CSF-stimulated *Mad1*$^{+/+}$ and *Mad1*$^{-/-}$ CFCs were classified on the basis of cell number per colony. *Mad1*$^{-/-}$ colonies were significantly larger in size (mean cell number/colony: *Mad1*$^{+/+}$, 117 ± 14; *Mad1*$^{-/-}$, 173 ± 17; n = 27 and 23, respectively; $P<0.02$). Similar results were obtained with GM-CSF. Data represent mean values ± SEM.

(Figure 3C). A similar expression pattern for *Mad1* mRNA has been observed during granulocytic differentiation of human HL-60 cells (Larsson *et al.*, 1994). We were unable to perform analogous experiments in primary cells since cluster-FCs cannot be purified to homogeneity; however,

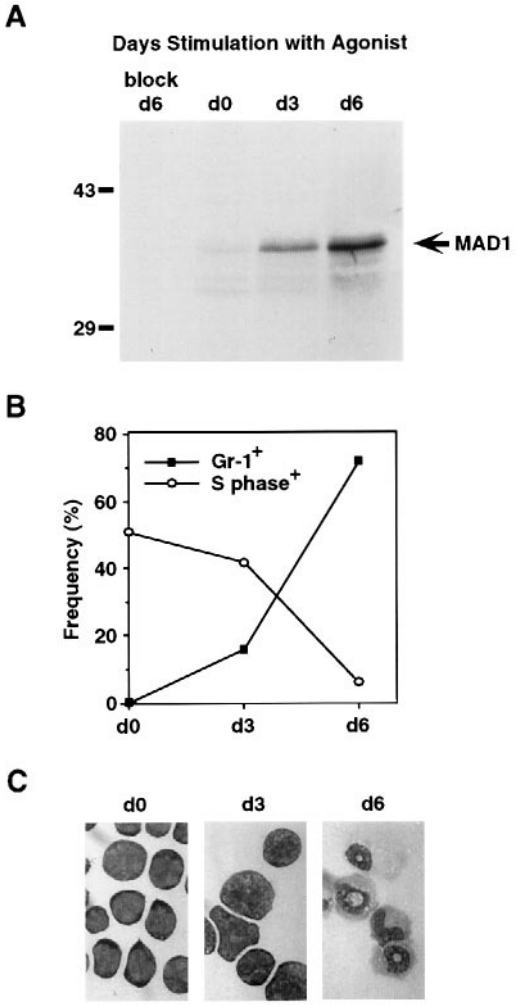

Fig. 3. MAD1 protein expression during granulocyte terminal differentiation. The murine MPRO cell line was induced to differentiate with 0.1 μM of an RXR agonist (see Materials and methods) for 0, 3 and 6 days (d). Following metabolic labeling with [^{35}S]methionine, anti-MAD1 immunoprecipitations were analyzed by 12.5% SDS–PAGE after normalizing to 4×10^6 cells/lane (**A**). Antisera was pre-blocked with peptide immunogen (block) to demonstrate the specificity of the MAD1 band. The positions of molecular weight markers (in kDa) are indicated to the left. The extent of terminal differentiation was monitored by determining the S-phase fraction and cell surface expression of Gr-1, both of which were detected by FACS analysis (**B**), and by morphology following staining with May–Grünwald Giemsa (**C**).

MAD1 is detectable in mature primary granulocytes by immunofluorescence (data not shown).

These results demonstrate that loss of MAD1 leads to an increased frequency of granulocytic cluster-FCs, without any change in the frequency of CFCs, the immediate precursors of cluster-FCs. However, as noted above, despite as much as a 3-fold increase in the frequency of granulocytic cluster-FCs in *Mad1*$^{-/-}$ mice, the frequency of terminally differentiated post-mitotic granulocytes in the bone marrow was only slightly elevated (Figure 2A and B), and was unaffected in the periphery (see Figure 6A below). This observation suggests that a compensatory mechanism must operate to maintain normal levels of mature cells in *Mad1*$^{-/-}$ animals despite the increase in cluster-FCs (see below).

Given the ability of ectopically expressed MAD1 to

inhibit cell cycle progression (Chen *et al.*, 1995; Roussel *et al.*, 1996), a reasonable hypothesis to explain these results would be that the increased cluster-FC frequency is due to a decreased ability of these cells to exit the cell cycle, which is a prerequisite for completion of terminal differentiation. To confirm these findings, we therefore examined the proliferative capacity of differentiating G- and GM-CSF-responsive precursors by labeling bone marrow cells with the intracellular fluorescent dye 5-(and -6)-carboxyfluorescein diacetate succinimidyl ester (CFSE), which allows the cumulative number of divisions which cells have undergone since labeling to be estimated due to the halving of fluorescence intensity that occurs with each division (Lyons and Parish, 1994). Following stimulation with G- or GM-CSF, *Mad1*$^{-/-}$ precursors were found to exhibit increased proliferation as terminal differentiation occurred (Figure 4A–D). Analogous results were also obtained by performing these experiments in the presence of 5-bromo-2′-deoxyuridine (BrdU) to label newly synthesized DNA (Figure 4E and F). Therefore, *Mad1*$^{-/-}$ granulocytic precursors undergo increased proliferation prior to becoming post-mitotic.

If this observed increase in cluster-FCs in *Mad1*$^{-/-}$ mice were cell autonomous, colonies derived from CFCs would be expected to produce more cluster-FCs, and hence be larger in size. Indeed, when bone marrow cells were stimulated with G-CSF at low cell density (to minimize the indirect effects of cell numbers on proliferation), *Mad1*$^{-/-}$ CFCs gave rise to colonies that were significantly larger in size than those derived from *Mad1*$^{+/+}$ littermates (Figure 2C). Consistent with this increase in cluster-FCs occurring *in vivo*, analysis of primary bone marrow cytospins revealed that the frequency of granulocytic precursors of promyelocyte/myelocyte morphology was increased in *Mad1*$^{-/-}$ animals (142 ± 19% relative to *Mad1*$^{+/+}$). Taken together, these results indicate that granulopoiesis in *Mad1*$^{-/-}$ mice is characterized by ectopic cell divisions occurring in a cell-autonomous fashion between the CFC and post-mitotic stages, resulting in delayed terminal differentiation.

Increased sensitivity of MAD1-deficient cells to cytokine withdrawal

As mentioned above, despite an increase in the number of granulocytic cluster-FCs in the bone marrow of *Mad1*$^{-/-}$ mice, the numbers of terminally differentiated post-mitotic granulocytes were almost unaffected (Figure 2A and B; also see Figure 6A below). One possible explanation for this disproportionality could be a compensatory decrease in cell survival. Bone marrow hematopoiesis is characterized by the generation of cells in considerable excess, resulting in extensive apoptotic cell death (McKenna and Cotter, 1997). This is particularly prevalent during the later stages of granulocyte differentiation, with >90% of bone marrow granulocytes failing to survive and exit into the periphery (Metcalf *et al.*, 1995). Apoptosis in the bone marrow is believed to be due in part to competition for the sub-maximal levels of cytokines present *in vivo*, and

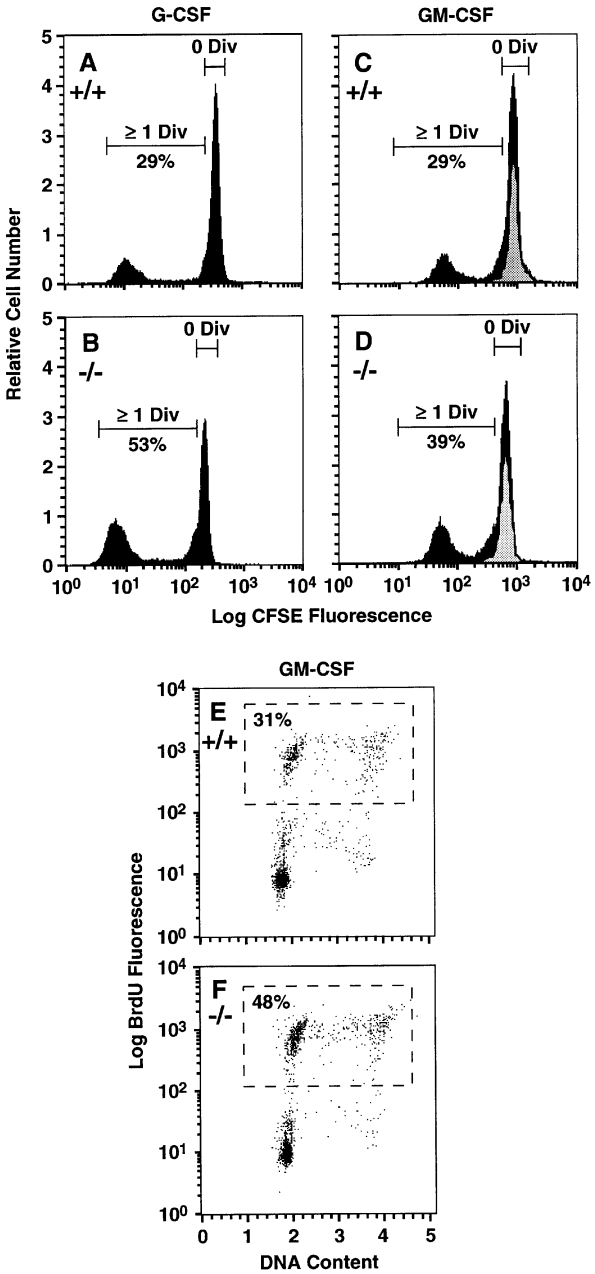

Fig. 4. Proliferative potential of bone marrow granulocytic precursors in *Mad1*$^{-/-}$ mice. (**A–D**) Representative FACS profiles of bone marrow cells from *Mad1*$^{+/+}$ (A and C) and *Mad1*$^{-/-}$ (B and D) mice ($n \geq 4$ for each genotype) labeled with CFSE and stimulated with 1000 U/ml G-CSF (A and B) or 1000 U/ml GM-CSF (C and D) in suspension cultures for 72 h. CFSE fluorescence decreases proportionally with the number of divisions undergone since labeling. For GM-CSF-stimulated cultures, CFSE fluorescence was gated on Gr-1^{+} cells. Cell division was blocked with colchicine in parallel cultures to establish the fluorescence signal (stippled area) of undivided cells (0 Div; C and D). The percentage of total cells in each culture that have divided at least once is also indicated (≥1 Div). *Mad1*$^{-/-}$ granulocyte precursors exhibited an increased proliferative fraction. CFSE staining of granulocytes resulted in the signal intensity being a continuum rather than the discrete peaks for each cell division previously observed for lymphocytes (Lyons and Parish, 1994). This is due to heterogeneity in granulocyte cell size resulting in the coefficient of variation (see width of 0 division peak) being much higher than for lymphocytes. (**E** and **F**) Representative FACS profiles of bone marrow cells from *Mad1*$^{+/+}$ (E) and *Mad1*$^{-/-}$ (F) mice ($n = 2$ for each genotype) metabolically labeled with BrdU and stimulated with 1000 U/ml GM-CSF for 72 h. Cells were stained with propidium iodide in order to detect relative DNA content. The area in the dashed boxes indicates the percentage of total cells that had entered the cell cycle and taken up BrdU. Wild-type (+/+); homozygous mutant (–/–); divisions (Div).

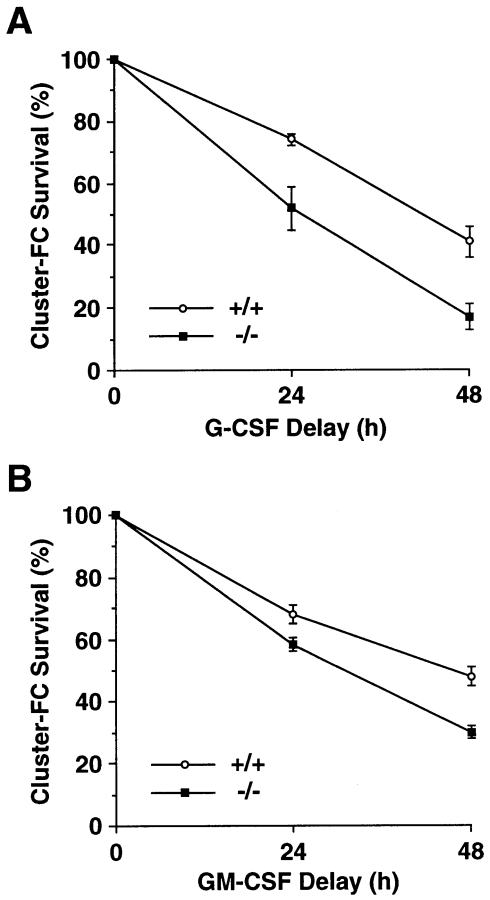

Fig. 5. Increased sensitivity of *Mad1*$^{-/-}$ hematopoietic cells to apoptosis-inducing conditions. Bone marrow cells from *Mad1*$^{+/+}$ (○) and *Mad1*$^{-/-}$ (■) mice were cultured in semi-solid media as in Figure 2, with the exception that 1000 U/ml G-CSF (**A**) or 1000 U/ml GM-CSF (**B**) were added only following 24 or 48 h of culture in the absence of cytokines. Cluster-FC survival (as a percentage of the maximum) following cytokine deprivation was significantly decreased in *Mad1*$^{-/-}$ animals ($P<0.05$ at 24 and 48 h). Data represent mean values ± SEM ($n \geqslant 3$ for each genotype). Wild-type (+/+); homozygous mutant (–/–).

hematopoietic cells are highly sensitive to undergoing apoptosis when deprived of such survival factors (McKenna and Cotter, 1997). To examine the sensitivity of *Mad1*$^{-/-}$ myeloid cells to apoptosis-inducing limiting cytokine conditions, *in vitro* clonogenic survival assays were performed in which cytokines were added following an initial period of culture in their absence. Delayed addition of G- or GM-CSF resulted in a significant decrease in cluster formation from *Mad1*$^{-/-}$ bone marrow with respect to that of control littermates, indicating that *Mad1*$^{-/-}$ granulocyte precursors exhibit decreased ability to survive under limiting cytokine conditions (Figure 5A and B). Continuous culture at intermediate cytokine concentrations resulted in a dose-dependent decrease in cluster-FC survival (data not shown). Consistent with these results, *Mad1*$^{-/-}$ granulocytic cluster-FCs also exhibited a 30–50% increased sensitivity to several other apoptosis-inducing stimuli, such as γ-irradiation and doxorubicin treatment (data not shown). Importantly, these effects were again restricted specifically to cluster-FCs, as the sensitivity of immature CFCs to cytokine withdrawal was unchanged in *Mad1*$^{-/-}$ animals. Similarly, the *in vivo* apoptosis of terminally differentiated post-mitotic cells (as measured by TUNEL or annexin V assays) and their *in vitro* survival under limiting cytokine conditions was also unchanged in *Mad1*$^{-/-}$ mice. These results suggest that the observed imbalance between the frequencies of granulocytic cluster-FCs and mature bone marrow and peripheral granulocytes is due to the decreased survival of cluster-FCs in *Mad1*$^{-/-}$ mice.

It is important to point out that it is not possible at present to examine apoptosis of cluster-FCs directly in *Mad1*$^{-/-}$ mice. This is due to the relative scarcity of granulocytic cluster-FCs as compared with terminally differentiated cells in the bone marrow, as well as the lack of available procedures to purify cluster-FCs to homogeneity. Furthermore, the rapid clearing of apoptotic granulocytes by phagocytosis results in only a small fraction being labeled in standard apoptosis assays (Metcalf *et al.*, 1995; Liu *et al.*, 1996). However, given that withdrawal of cytokines from primary hematopoietic cells and non-transformed hematopoietic cell lines invariably results in apoptotic cell death (McKenna and Cotter, 1997), it is likely that the decreased survival of *Mad1*$^{-/-}$ granulocytic cluster-FCs *in vitro* is due to an increased rate of apoptosis.

Enhanced recovery of Mad1 null mice following bone marrow ablation

These observations suggest that homeostatic compensation for delayed granulocyte differentiation in *Mad1*$^{-/-}$ mice is due to a cell-autonomous decrease in cell survival, resulting in essentially normal numbers of mature bone marrow and circulating peripheral blood granulocytes. To examine granulopoiesis in *Mad1*$^{-/-}$ animals under conditions where the hematopoietic compartment is not at a steady-state equilibrium, proliferating bone marrow precursors were ablated by i.v. injection of 5-fluorouracil (5-FU). Suppression of hematopoiesis following this treatment occurred to a similar extent in *Mad1*$^{-/-}$ and *Mad1*$^{+/+}$ mice (Figure 6A). Strikingly, however, by 14 days following 5-FU treatment the mature peripheral blood and splenic granulocytes had recovered to significantly higher levels in *Mad1*$^{-/-}$ than *Mad1*$^{+/+}$ mice (Figure 6A and B). Similarly, increased numbers of granulocytic cluster-FCs were observed in the bone marrow and spleen of *Mad1*$^{-/-}$ animals (Figure 6C). As described above, this is in contrast to the normal numbers of mature splenic and peripheral blood granulocytes observed in untreated *Mad1*$^{-/-}$ animals. This effect was again stage specific as there was no significant difference in number of more immature bone marrow CFCs. These results are consistent with *Mad1*$^{-/-}$ mice having a larger granulocyte cluster-FC pool due to delayed terminal differentiation, and suggest that the compensatory decrease in survival of cluster-FCs observed in *Mad1*$^{-/-}$ mice is over-ridden during recovery from granulocytopenia.

Mad gene family redundancy in Mad1 knockout mice

In contrast to the inhibition of cell cycle exit during granulocyte differentiation in *Mad1*$^{-/-}$ mice, other hematopoietic cell types were less obviously affected. For example, *Mad1*$^{-/-}$ mice exhibited a small increase in the frequency of low proliferative-potential erythroid and

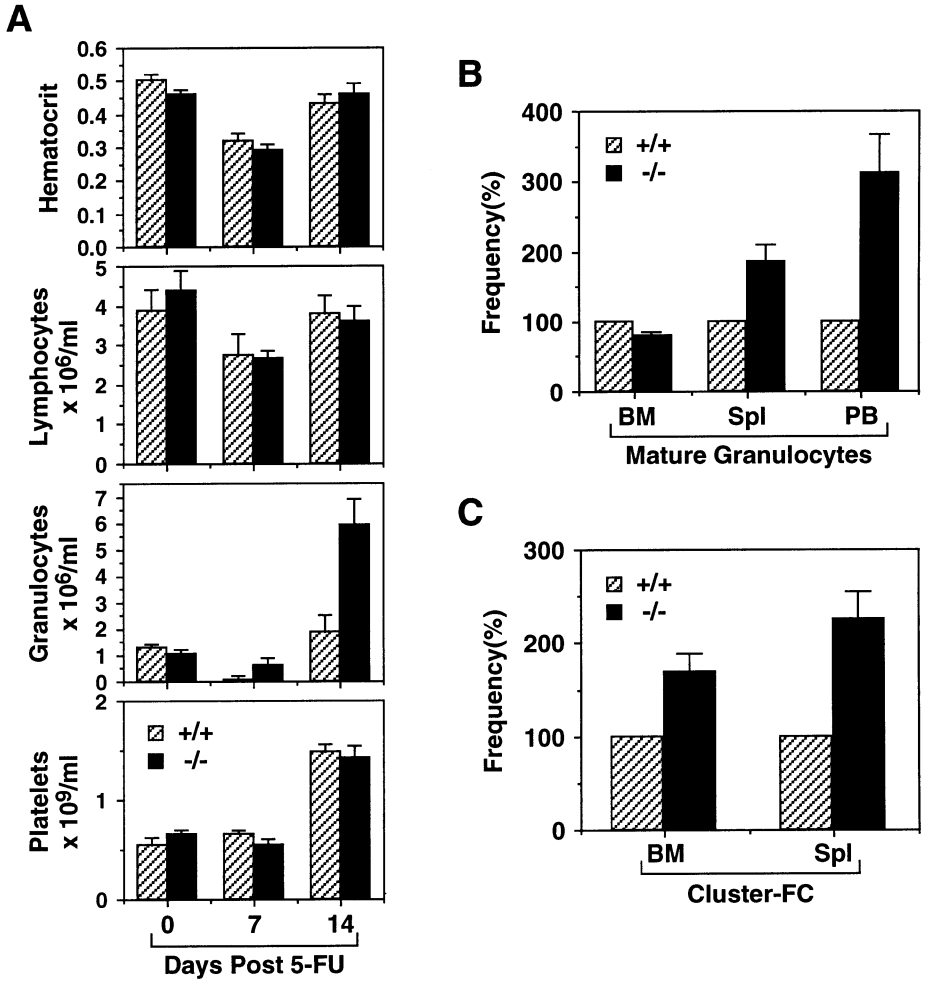

Fig. 6. Recovery of the granulocytic lineage in *Mad1*$^{-/-}$ mice following bone marrow ablation. Bone marrow ablation was performed in *Mad1*$^{-/-}$ ($n = 4$) and *Mad1*$^{+/+}$ ($n = 4$) mice by i.v. injection of 5-FU. Peripheral blood counts and smears were performed on intra-orbital blood on days 0, 7 and 14 following 5-FU injection (**A**). The frequency of Gr-1^{+} mature granulocytes was determined by FACS on day 14 (**B**), and the frequency of G-CSF responsive cluster-FCs was determined as in Figure 2C (**C**). Peripheral granulocytes and cluster-FC reached significantly higher levels in *Mad1*$^{-/-}$ animals relative to controls ($P<0.05$). Mature bone marrow granulocytes in wild-type and mutant mice returned to approximately steady-state levels by day 14 (B). On day 7 following 5-FU treatment (A), circulating granulocytes were suppressed to an identical extent in the *Mad1*$^{+/+}$ controls and two of four *Mad1*$^{-/-}$ animals. Although two other *Mad1*$^{-/-}$ animals exhibited slightly higher numbers, this difference did not affect the extent of recovery observed on day 14. Data represent mean values ± SEM. Peripheral blood (PB); bone marrow (BM); red blood cell (RBC); spleen (S).

macrophage precursors (~120% of wild-type; $P<0.05$), and the survival of these cells following delayed addition of erythropoietin (Epo) or macrophage colony-stimulating factor (M-CSF) was also reduced (~70% of wild-type; $P<0.05$). Additionally, *Mad1*$^{-/-}$ resting B lymphocytes were found to re-enter the cell cycle significantly more rapidly than wild-type cells, as determined by BrdU labeling following *in vitro* stimulation with mitogenic bacterial lipopolysaccaride (LPS) (fraction labeled after 48 h: *Mad1*$^{+/+}$, 28.0 ± 1.7%; *Mad1*$^{-/-}$, 37.8 ± 1.7%; $P<0.01$). This suggests that MAD1 may play a role in cell cycle arrest of mature B cells, although *Mad1*$^{-/-}$ mice produced normal levels of serum immunoglobulins and were not prone to spontaneous infection when housed under non-pathogen-free conditions. However, by histology, other tissues appeared to differentiate normally, and a careful examination of neural differentiation did not reveal any evidence for ectopic mitosis, delayed differentiation or decreased cell survival.

The restriction of the *Mad1*$^{-/-}$ phenotype primarily to the granulocytic lineage may be explained by the fact that *Mad1* is one of four members of the *Mad* gene family, each of which is expressed in overlapping but distinct patterns (Hurlin *et al.*, 1995b; Quéva *et al.*, 1998). Although MAD1 is the most extensively studied family member, other MADs appear to behave similarly *in vitro* and in tissue culture systems (Hurlin *et al.*, 1995b). Hence, there is considerable potential for genetic redundancy among the *Mad* family. Functional compensation might also occur through up-regulation of other MAD family members in the absence of MAD1. To address this possibility, mRNA *in situ* hybridizations were performed to examine the expression patterns of other members of the *Max* network in *Mad1*$^{-/-}$ mice. Two *Mad1*-related genes were found to be ectopically expressed in the spleens of *Mad1*$^{-/-}$ animals: *Mxi1* was induced in the red pulp surrounding lymphoid follicles (Figure 7C and D); and *Mad3* was up-regulated in lymphoid germinal centers (Figure 7E and F). Both these regions normally express high levels of *Mad1* (Figure 7A). However, there were no

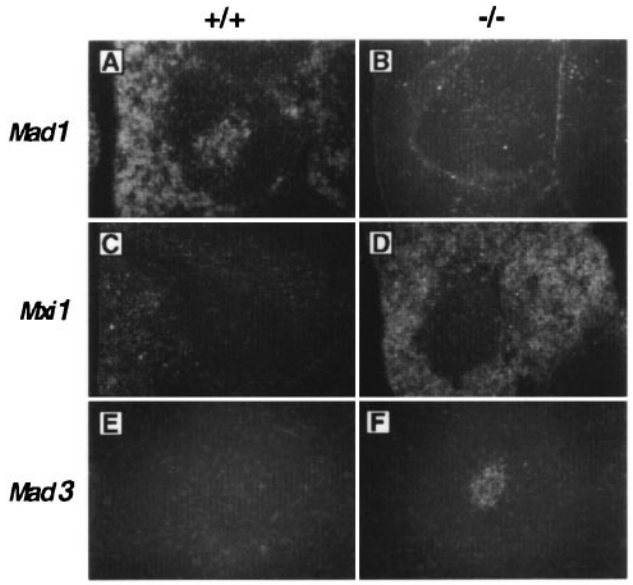

Fig. 7. Altered expression of the *Mad* gene family in *Mad1*$^{-/-}$ mice. (A–F) mRNA *in situ* hybridizations for *Mad1* (**A** and **B**), *Mxi1* (**C** and **D**) and *Mad3* (**E** and **F**) expression were performed on paraffin-sectioned spleens from adult *Mad1*$^{+/+}$ (A, C and E) and *Mad1*$^{-/-}$ (B, D and F) mice with antisense riboprobes. Darkfield photography was performed so that a single lymphoid follicle with a central germinal center is positioned in the middle of each image and surrounded by red pulp. *Mxi1* and *Mad3* were up-regulated in the red pulp and germinal centers of *Mad1*$^{-/-}$ mice, respectively. Wild-type (+/+); homozygous mutant (–/–).

appreciable changes in c-*Myc*, N-*Myc*, *Max* or *Mad4* expression in the spleen, and no obvious alterations in expression of the *Mad* gene family in a number of other tissues. These results suggest that the *Mad* gene family may be transcriptionally cross-regulated.

Discussion

It is well established that cell cycle withdrawal and terminal differentiation are tightly coupled processes in most cell types. The G_0/G_1 arrest of cells prior to terminal differentiation typically requires down-regulation of MYC expression (Coppola and Cole, 1986; Freytag, 1988). With the concomitant up-regulation of MAD1, this leads to MYC–MAX complexes being replaced rapidly by MAD1–MAX complexes (Ayer and Eisenman, 1993; Hurlin *et al.*, 1995b; Cultraro *et al.*, 1997). Given the ability of ectopically expressed MAD1 to promote G_1 arrest and antagonize MYC-dependent transcription and transformation (see Introduction), we have proposed that induction of MAD1 plays an important role in mediating cell cycle withdrawal during terminal differentiation.

To test this hypothesis, we generated targeted disruptions of the *Mad1* gene in mice. Although *Mad1*$^{-/-}$ mice were viable and outwardly normal in appearance, we found that cell cycle exit of granulocytic precursors was delayed following the CFC stage, as evidenced by an increased number of cell divisions occurring between the CFC and post-mitotic stages of differentiation. This conclusion is based on both the increased frequency of cluster-FCs detected *in vivo* and the enhanced proliferative capacity of CFCs measured *in vitro*. In contrast, the number of terminally differentiated granulocytes was found to be largely unaffected in *Mad1*$^{-/-}$ mice. We did find, however, that granulocytic cluster-FCs exhibited increased sensitivity to apoptosis-inducing conditions, raising the possibility that decreased cell survival accounts for the observed imbalance between precursor and mature granulocytes during steady-state hematopoiesis *in vivo*. Further, *Mad1*$^{-/-}$ mice exhibited enhanced recovery of peripheral granulocyte populations following bone marrow ablation, probably reflecting the increased proliferative capacity of CFCs in these animals. Taken together, these results provide the first direct demonstration that MAD1 functions to mediate cell cycle withdrawal during terminal differentiation, and also suggest that competition between MYC and MAD1 regulates a balance between granulocyte proliferation and terminal differentiation.

The oncogenic activation of MYC typically is associated with its overexpression (Marcu *et al.*, 1992). For example, Eμ-*Myc* transgenic mice that ectopically express MYC during B cell development are highly predisposed to lymphomas (Morgenbesser and DePinho, 1994). Interestingly, prior to the onset of neoplasia in Eμ-*Myc* mice, B cell development is characterized by increased proliferation and apoptosis of pre-B cells at the expense of their further differentiation (Langdon *et al.*, 1986; Jacobsen *et al.*, 1994). The phenotypes of *Mad1*$^{-/-}$ and pre-neoplastic Eμ-*Myc* mice, although affecting different cell lineages, are similar to one another, consistent with the suggestion that MYC and MAD1 have mutually antagonistic roles in cell proliferation and differentiation, and that the MYC signaling pathway is deregulated in *Mad1* knockout mice.

Ectopic expression of MAD1 has been shown to inhibit cell transformation, raising the possibility that it functions as a tumor suppressor *in vivo* (Lahoz *et al.*, 1994). However, in contrast to the development of lymphomas in Eμ-*Myc* mice, *Mad1*$^{-/-}$ mice do not exhibit an increased rate of spontaneous neoplasia. This observation suggests that MYC activity may not be deregulated sufficiently to promote tumorigenesis in *Mad1*$^{-/-}$ mice, or alternatively that granulocytic cluster-FCs are resistant to transformation by MYC. However, it is also possible that tumors may develop in *Mad1*$^{-/-}$ mice only following a long latency period, and that different genetic backgrounds or other cooperating mutations may be required to potentiate tumor formation.

Given the broad expression pattern of the *Mad1* gene, it is perhaps surprising that *Mad1*$^{-/-}$ animals do not exhibit more generalized defects in cell differentiation. This may be explained in part by functional redundancy between MAD1 and other members of the MAD family, as has been seen recently with other multigene families (Lowell and Soriano, 1996; Molkentin and Olson, 1996; Zhuang *et al.*, 1996). Furthermore, we have observed that *Mxi1* and *Mad3* are up-regulated in *Mad1*$^{-/-}$ mice, suggesting that compensation might also occur through transcriptional cross-regulation of the *Mad* gene family. This finding is similar to the previously reported up-regulation of c-*Myc* in neural cells of N-*Myc* knockout mice (Stanton *et al.*, 1992), and may indicate the existence of feedback controls for maintaining the appropriate cellular balance between MYCs and MADs. Targeted disruptions of other *Mad* genes and the generation of double knockout mice will be required to resolve fully the extent of redundancy among the MAD family.

Commitment to terminal differentiation is likely to be regulated by the convergence of multiple independent regulatory pathways. Thus it is possible that MAD1 acts cooperatively with other unrelated cell cycle inhibitors to promote differentiation. For example, targeted disruption of the retinoblastoma protein RB in mice inhibits terminal differentiation of several cell lineages (Clarke *et al.*, 1992; Jacks *et al.*, 1992; Lee *et al.*, 1992, 1994; Morgenbesser *et al.*, 1994; Zacksenhaus *et al.*, 1996). Interestingly, RB also appears to function in maintaining cells in the G_0 phase of the cell cycle following completion of terminal differentiation (Lee *et al.*, 1994; Schneider *et al.*, 1994; Zacksenhaus *et al.*, 1996). In contrast, mature Gr-1$^+$ granulocytes from *Mad1*$^{-/-}$ mice are incapable of re-entering the cell cycle when stimulated with G- and/or GM-CSF (data not shown). This difference between *Rb*$^{-/-}$ and *Mad1*$^{-/-}$ cells may be related to the inability of MYC to induce proliferation in some terminally differentiated cells (Endo and Nadal-Ginard, 1986).

The CIP/KIP family of cyclin-dependent kinase inhibitors (CKIs) have also been implicated in terminal differentiation. In this regard, it is intriguing that the phenotype of *Mad1*$^{-/-}$ mice is similar to those observed due to null mutations in the CKIs *Drosophila* Dacapo, and murine p21^{CIP1}, p27^{KIP1} and p57^{KIP2} (de Nooij *et al.*, 1996; Lane *et al.*, 1996; Missero *et al.*, 1996; Casaccia-Bonnefil *et al.*, 1997; Yan *et al.*, 1997; Zhang *et al.*, 1997). All of these mutations lead to delayed terminal differentiation of specific tissues due to low proliferative potential precursors undergoing one or more ectopic divisions prior to cell cycle arrest. The similarity of these phenotypes raises the possibility that these pathways cooperate to mediate cell cycle withdrawal during differentiation, or that there are previously unrecognized epistatic relationships between them.

During development, many examples of programed cell death appear to result from competition between cells for limiting survival factors (Raff, 1992). The decreased survival of *Mad1*$^{-/-}$ granulocytic cluster-FCs under cytokine-limiting conditions suggests that MAD1 may function in part to regulate the sensitivity of cells to MYC-induced apoptosis. Since MAD1 deficiency results in both inhibition of terminal differentiation and decreased cell survival, it is tempting to speculate that both these effects result from a delay in the down-regulation of proliferation-associated genes during terminal differentiation. Interestingly, inhibition of terminal differentiation in RB-deficient mice is also associated with ectopic cell death in several tissues (Lee *et al.*, 1994; Morgenbesser *et al.*, 1994; Macleod *et al.*, 1996; Zacksenhaus *et al.*, 1996), and induction of p21^{CIP1} during differentiation of myoblast and neuroblastoma cell lines has also been found to enhance cell survival (Poluha *et al.*, 1996; Wang and Walsh, 1996). Therefore, deregulation of cell cycle exit may generally increase the probability of cell death due to an imbalance between signals promoting cell proliferation (MYC and cyclin-dependent kinases) and other signals promoting differentiation (MAD, RB and CKIs). Alternatively, these genes may directly regulate signaling pathways that mediate cell survival and which are entirely independent of cell proliferation pathways. The combinatorial expression patterns of MYCs, MADs and other cell cycle regulators probably play an important role in providing the diversity of cell numbers that is observed among different tissues and under different environmental conditions, by balancing proliferation, differentiation and cell survival. Detailed analysis of the gene expression patterns in MAD1-deficient cells may provide further insights into these questions.

Materials and methods

Construction of targeting vectors

A human *Mad1* cDNA (Ayer *et al.*, 1993) was employed to screen a murine AB1 ES cell cDNA library (Chen *et al.*, 1994). One of two independent clones was sequenced and found to contain the entire open reading frame of *Mad1* (DDBJ/EMBL/GenBank accession No. U20614). This cDNA was used to screen a murine 129/Sv genomic library (G.Friedrich and P.Soriano, unpublished), and the resulting clones were restriction mapped and sequenced for confirmation. A 5.3 kb *Sal*I–*Xho*I fragment (Figure 1A) containing the 5′ end of the *Mad1* gene (including the promoter and exons 1 and 2) was employed to create two different targeting vectors: (i) p*Mad1*^{tm1} (Figure 1A), in which a 318 bp *Sac*II–*Not*I fragment (encompassing the proximal *Mad1* promoter, first exon and 29 bp of the first intron) was replaced by a PGK*neo*bpA cassette, oriented in the opposite transcriptional direction to *Mad1*; and (ii) p*Mad1*^{tm2}, which will be described in detail elsewhere (K.P.Foley, unpublished). In both constructs, the negative selectable marker cassette, PGK*tk*pA, was introduced between the plasmid backbone and *Mad1* 'short arm'. Mock PCR-positive control versions of each vector were generated by replacing the PGK*tk*pA cassette with a 1.75 kb *Eco*RI–*Xho*I fragment from the *Mad1* second intron in its normal orientation.

ES cell procedures

ES cells were manipulated essentially as previously described (Soriano *et al.*, 1991). Passage 10 AK7 ES cells derived from the 129/Sv mouse strain (A.Imamoto and P.Soriano, unpublished) were cultured on mitomycin C-inactivated, leukemia inhibitory factor-expressing SNL 76/7 feeder cells, electroporated with *Sal*I-linearized targeting vectors and placed under positive/negative selection with G418 and FIAU. ES cell colonies surviving after 9 days were analyzed by PCR using the following oligonucleotide primers: K15 (antisense 3′ primer derived from *Mad1* second intron; Figure 1A), 5′-CCAACAGCCACGGAAGAGAT-3′; K16 (5′ sense primer derived from PGK promoter in p*Mad1*^{tm1}; Figure 1A), 5′-GAGCCCAGAAAGCGAAGGAG-3′; and K21 (5′ sense primer derived from polylinker sequence in p*Mad1*^{tm2}; not shown), 5′-GTCTGGATCCCCTCGACCTC-3′. Mock targeting vectors (described above) were used initially to establish PCR assay conditions capable of detecting 1 fg of mock target in a background 100 ng of genomic DNA after 40 cycles. These conditions previously have been determined to provide sufficient sensitivity to detect one homologous recombinant ES cell clone in a pool of >10 non-homologous recombinants (P.Soriano, unpublished). Between 10 and 20% of each ES cell colony was picked individually or in pools, and lysed in 12 μl of PCR lysis buffer [1× PCR buffer (described below), 1.7 mM SDS, 50 μg/ml proteinase K] by heating at 37°C for 1 h and then at 85°C for 10 min. Aliquots (5 μl) of lysate were amplified in 25 μl PCR reactions containing 1× MGB II [16.6 mM $(NH_4)_2SO_4$, 67 mM Tris (pH 8.8), 6.5 mM $MgCl_2$, 1 mM each dNTP, 10% dimethyl sulfoxide, 1% β-mercaptoethanol (βME), 0.01% gelatin; A.Imamoto and P.Soriano, unpublished), 2.5 pmol of each appropriate primer (K15 and K16 for *Mad1*^{tm1}, and K15 and K21 for *Mad1*^{tm2}], 2.5 U of *Taq* DNA polymerase and 2.5 U of *Taq* Extender (Stratagene). PCR reactions were performed with the following temperature profiles: an initial denaturation at 95°C for 5 min, then 40 repeating cycles of 93°C for 35 s, 50°C (for *Mad1*^{tm1}) or 55°C (for *Mad1*^{tm2}) for 40 s, and 65°C for 3 min 50 s.

Clones were analyzed by Southern blotting with probes diagnostic for the 5′ (probe A) and 3′ (probe B) ends of the expected homologous recombination events (Figure 1A), and for the *neo* and *tk* selectable markers (not shown). Fifteen μg of *Xba*I-digested genomic DNA was electrophoresed on a 0.8% agarose gel, treated with 0.25 M HCl for 15 min and blotted to Hybond-N+ membrane (Amersham) by capillary transfer in 0.4 M NaOH for 3 h. Hybridizations were performed at 65°C for 12 h in FBI buffer (1.5× SSPE, 7% SDS, 10% polyethylene glycol 8000, 100 mg/ml sonicated and boiled salmon sperm DNA), and blots were washed three times at 65°C (in 0.1× SSC, 0.1% SDS) before autoradiography.

ES cell clones were injected into C57BL/6 blastocysts and then transplanted into pseudopregnant females following standard procedures. Nine out of nine clones gave rise to chimeric founders that transmitted the targeted alleles through the germ line. Progeny were genotyped by PCR (as above, but using 50 ng of genomic tail DNA and 27 cycles), heterozygous siblings were interbred, and the resulting F_2 generation analyzed by Southern blotting. Most experiments were performed using 8- to 12-week-old *Mad1*$^{+/+}$ and *Mad1*$^{-/-}$ littermates.

mRNA and protein expression analysis

Total RNA was prepared from adult mouse tissues with TRIzol Reagent (Gibco BRL) following the manufacturer's instructions. RT–PCR assays were performed essentially as previously detailed (Leonard *et al.*, 1993) by independently amplifying cDNA with control primers specific for the murine ribosomal protein S16 mRNA, and the following *Mad1* primers (63°C annealing temperature): sense exons 5/6 junction, 5′-CTCTGATAGAGAAGAACTGGACG-3′; and antisense exon 6, 5′-TCGTCCGAGTCACTCACGCTG-3′. Radiolabeled amplification products were electrophoresed on denaturing sequencing gels and visualized by autoradiography.

MPRO cells were cultured as described (Tsai and Collins, 1993). Differentiation was induced with an RXR agonist, ALGN 19204 (Allergan). This compound is a potent inducer of terminal differentiation of the MPRO cell line (S.Collins, personal communication). MAD1 protein expression was analyzed by radioimmunoprecipitation with anti-human MAD1 polyclonal antisera #C19 (Santa Cruz), essentially as detailed (Blackwood *et al.*, 1992).

Expression of the murine c-*Myc*, N-*Myc*, *Max*, *Mad1*, *Mxi1*, *Mad3* and *Mad4* genes was analyzed by mRNA *in situ* hybridization using ^{35}S-labeled riboprobes probes, as previously described (Hurlin *et al.*, 1995b).

Flow cytometry

Immunostaining was performed by pre-incubating single cell suspensions with anti-Fc receptor antibody 24G.2, followed by incubation with lineage-specific antibodies and 1 μg/ml 7-amino actinomycin-D (Molecular Probes), and analyzed on a FACScan (Becton Dickinson). The following biotin-, fluorescein (FITC)- and phycoerythrin (PE)-labeled antibodies and reagents were employed: biotin–anti-B220, biotin–anti-CD34, FITC–anti-Gr-1, FITC–anti-IgM and biotin–anti-Ter119 (Pharmigen); biotin–anti-CD4, FITC–anti-CD8, biotin–anti-c-Kit, PE–anti-F4/80, PE–anti-Mac1/CD11b, streptavidin–PE and streptavidin–FITC (Caltag). Statistical analyses for all hematopoietic cell studies were performed using a two-sided unpaired Student's *t*-test.

Hematopoietic cell culture

All cultures were performed in a 37°C/5% CO_2 fully humidified incubator. Clonal myeloid cultures were performed as previously described (Metcalf, 1984). Briefly, 2.5×10^4 bone marrow or splenic cells were stimulated in 1 ml of semi-solid media containing 0.3% agar and 20% calf serum (CS; Hyclone) in Dulbecco's modified Eagle's medium (DMEM). After 2 and 7 days, the number of clonogenic cells was determined by stereomicroscopy. Differential counts and determination of colony size were performed on fixed cultures after staining for acetylcholinesterase activity followed by luxol fast-blue and hematoxylin. Clonal erythroid cultures were performed as previously detailed (Metcalf, 1984). The erythroid nature of colonies was confirmed by staining with acid-benzidene. The following recombinant cytokines were employed: Epo and G-CSF (Amgen); GM-CSF, partially purified interleukin (IL)-3, IL-6 and stem cell factor (Immunex); and M-CSF baculovirus supernatant (L.Rohrschneider). To analyze the effects of cytokine starvation, cytokines were omitted from clonal myeloid and erythroid cultures during the first 24–48 h and then added back by evenly distributing the appropriate quantity of cytokines over the surface of the cultures in 0.2 ml of media.

Cell cycle analysis

To analyze granulocyte precursor cell proliferation, 1×10^5 bone marrow cells/ml were stimulated in suspension with 1000 U/ml G-CSF or GM-CSF (in DMEM containing 20% CS), and cultured in the presence of 10 μM BrdU (Sigma) for 72 h prior to harvesting. Alternatively, cells were labeled with 10 μM CFSE (Molecular Probes). In the latter case, to indicate the fluorescence level of undivided cells, 2 μM colchicine (Sigma) was added following labeling with CFSE. Similarly, to analyze cell proliferation of mature B lymphocytes, 1×10^6 splenocytes were stimulated with 20 μg/ml *Escherichia coli* LPS (Sigma) in 1 ml of suspension culture (in RPMI 1640 media containing 10% fetal bovine serum, 10 mM L-glutamine and 50 μM βME). BrdU was added after 16 h, and cells were harvested after 24–72 h. Following BrdU labeling, granulocytes and B lymphocytes were fixed with 86% ethanol in phosphate-buffered saline (PBS), and then stained with anti-BrdU antibody (Becton Dickinson) and FITC-conjugated goat anti-mouse IgG (Capel) according to the manufacturer's protocols. After staining with 10 μg/ml propidium iodide (PI) (in PBS containing 2% CS), cells were analyzed on a FACScan. The S-phase fraction of MPRO cells was determined by PI staining as above, but including 0.25 mg/ml RNase A.

Bone marrow chemo-ablation

Injections of 5-FU (Sigma) at 150 μg/g body weight (in PBS) were performed via the tail vein. Differential counts and peripheral blood smears were performed from intra-orbital blood on days 7 and 14 following injection. Animals were sacrificed on day 14, mature granulocyte numbers determined by FACS, and granulocytic precursors assayed *in vitro* as described above.

Acknowledgements

We thank D.Ayer, A.Berger, A.Bush, Z.Chen, S.Collins, S.Fiering, G.Friedrich, A.Imamoto, B.Johnston, T.Knight, T.Pounder, L.Purton, L.Ramos, L.Rohrschneider, G.Sale, P.Stein, D.Tarlington, B.Zambrowicz and Y.Zhuang for advice, assistance or reagents. We also thank S.Collins and J.Roberts for critical comments on the manuscript. GM-CSF, IL-3, IL-6 and SCF were generously provided by Immunex Corp. This work was supported by fellowships from the American Cancer Society (PF-4103 to K.P.F.) and the Damon Runyon–Walter Winchell Foundation (DRG 076 to G.A.M.) and by grants from the National Institutes of Health (R01CA57138 and HL54881 to R.N.E.; HD 25326 and HD24875 to P.S.). R.N.E is an American Cancer Society Research Professor.

References

Alland,L., Muhle,R., Hou,Jr.H., Potes,J., Chin,L., Schreiber-Agus,N. and DePinho,R.A. (1997) Role for N-CoR and histone deacetylase in Sin3-mediated transcriptional repression. *Nature*, **387**, 49–55.

Amati,B., Dalton,S., Brooks,M.W., Littlewood,T.D., Evan,G.I. and Land,H. (1992) Transcriptional activation by the human c-Myc oncoprotein in yeast requires interaction with Max. *Nature*, **359**, 423–426.

Askew,D.S., Ashmun,R.A., Simmons,B.C. and Cleveland,J.L. (1991) Constitutive c-*myc* expression in an IL-3-dependent myeloid cell line suppresses cell cycle arrest and accelerates apoptosis. *Oncogene*, **6**, 1915–1922.

Ayer,D.E. and Eisenman,R.N. (1993) A switch from Myc:Max to Mad:Max heterocomplexes accompanies monocyte/macrophage differentiation. *Genes Dev.*, **7**, 2110–2119.

Ayer,D.E., Kretzner,L. and Eisenman,R.N. (1993) Mad: a heterodimeric partner for Max that antagonizes Myc transcriptional activity. *Cell*, **72**, 211–222.

Ayer,D.E., Lawrence,Q.A. and Eisenman,R.N. (1995) Mad–Max transcriptional repression is mediated by ternary complex formation with mammalian homologs of yeast repressor Sin3. *Cell*, **80**, 767–776.

Blackwood,E.M. and Eisenman,R.N. (1991) Max: a helix–loop–helix zipper protein that forms a sequence-specific DNA-binding complex with Myc. *Science*, **251**, 1211–1217.

Blackwood,E.M., Lüscher,B. and Eisenman,R.N. (1992) Myc and Max associate *in vivo*. *Genes Dev.*, **6**, 71–80.

Casaccia-Bonnefil,P., Tikoo,R., Kiyokawa,H., Friedrich,V.,Jr, Chao,M.V. and Koff,A. (1997) Oligodendrocyte precursor differentiation is perturbed in the absence of the cyclin-dependent kinase inhibitor p27^{Kip1}. *Genes Dev.*, **11**, 2335–2346.

Cerni,C., Bousset,K., Seelos,C., Burkhardt,H., Henriksson,M. and Lüscher,B. (1995) Differential effects by Mad and Max on transformation by cellular and viral oncoproteins. *Oncogene*, **11**, 587–596.

Chen,J., Willingham,T., Margraf,L.R., Schreiber-Agus,N., DePinho,R.A. and Nisen,P.D. (1995) Effects of the *MYC* oncogene antagonist, MAD, on proliferation, cell cycling and the malignant phenotype of human brain tumor cells. *Nature Med.*, **1**, 638–643.

Chen,Z., Friedrich,G.A. and Soriano,P. (1994) Transcriptional enhancer factor 1 disruption by a retroviral gene trap leads to heart defects and embryonic lethality in mice. *Genes Dev.*, **8**, 2293–2301.

Chin,L., Schreiber-Agus,N., Pellicer,I., Chen,K., Lee,H.-W., Dudast,M., Cordon-Cardo,C. and DePinho,R.A. (1995) Contrasting roles for Myc

and Mad proteins in cellular growth and differentiation. *Proc. Natl Acad. Sci. USA*, **92**, 8488–8492.
Clarke,A.R., Maandag,E.R., van Roon,M., van der Lugt,N.M.T., van der Valk,M., Hooper,M.L., Berns,A. and te Riele,H. (1992) Requirement for a functional *Rb-1* gene in murine development. *Nature*, **359**, 328–330.
Coppola,J.A. and Cole,M.D. (1986) Constitutive c-*myc* oncogene expression blocks mouse erythroleukaemia cell differentiation but not commitment. *Nature*, **320**, 760–763.
Cultraro,C.M., Bino,T. and Segal,S. (1997) Function of the c-Myc antagonist Mad1 during a molecular switch from proliferation to differentiation. *Mol. Cell. Biol.*, **17**, 2353–2359.
Delgado,M.D., Lerga,A., Cañelles,M., Gómez-Casares,M.T. and León,J. (1995) Differential regulation of Max and role of c-Myc during erythroid and myelomonocytic differentiation of K562 cells. *Oncogene*, **10**, 1659–1665.
de Nooij,J.C., Letendre,M.A. and Hariharan,I.K. (1996) A cyclin-dependent kinase inhibitor, Dacapo, is necessary for timely exit from the cell cycle during *Drosophila* embryogenesis. *Cell*, **87**, 1237–1247.
Eilers,M., Schirm,S. and Bishop,J.M. (1991) The MYC protein activates transcription of the α-prothymosin gene. *EMBO J.*, **10**, 133–141.
Endo,T. and Nadal-Ginard,B. (1986) Transcriptional and posttranscriptional control of c-*myc* during myogenesis: its mRNA remains inducible in differentiated cells and does not suppress the differentiated phenotype. *Mol. Cell. Biol.*, **6**, 1412–1421.
Evan,G.I., Wyllie,A.H., Gilbert,C.S., Littlewood,T.D., Land,H., Brooks,M., Waters,C.M., Penn,L.Z. and Hancock,D.C. (1992) Induction of apoptosis in fibroblasts by c-myc protein. *Cell*, **69**, 119–128.
Freytag,S.O. (1988) Enforced expression of the c-*myc* oncogene inhibits cell differentiation by precluding entry into a distinct predifferentiation state in G_0/G_1. *Mol. Cell. Biol.*, **8**, 1614–1624.
Gandarillas,A. and Watt,F.M. (1995) Changes in expression of members of the *fos* and *jun* families and *myc* network during terminal differentiation of human keratinocytes. *Oncogene*, **11**, 1403–1407.
Grandori,C. and Eisenman,R.N. (1997) Myc target genes. *Trends Biochem. Sci.*, **22**, 177–181.
Hassig,C.A., Fleischer,T.C., Billin,A.N., Schreiber,S.L. and Ayer,D.E. (1997) Histone deacetylase activity is required for full transcriptional repression by mSin3A. *Cell*, **89**, 341–347.
Heikkila,R., Schwab,G., Wickstrom,E., Loke,S.L., Pluznik,D.H., Watt,R. and Neckers,L.M. (1987) A c-*myc* antisense oligodeoxynucleotide inhibits entry into S phase but not progress from G_0 to G_1. *Nature*, **328**, 445–449.
Heinzel,T. *et al*. (1997) A complex containing N-CoR, mSin3 and histone deacetylase mediates transcriptional repression. *Nature*, **387**, 43–48.
Henriksson,M. and Lüscher,B. (1996) Proteins of the Myc network: essential regulators of cell growth and differentiation. *Adv. Cancer Res.*, **68**, 109–182.
Hurlin,P.J., Foley,K.P., Ayer,D.E., Eisenman,R.N., Hanahan,D. and Arbeit,J.M. (1995a) Regulation of Myc and Mad during epidermal differentiation and HPV-associated tumorigenesis. *Oncogene*, **11**, 2487–2501.
Hurlin,P.J., Quéva,C., Koskinen,P.J., Steingrimsson,E., Ayer,D.E., Copeland,N.G., Jenkins,N.A. and Eisenman,R.N. (1995b) Mad3 and Mad4: novel Max-interacting transcriptional repressors that suppress c-*myc* dependent transformation and are expressed during neural and epidermal differentiation. *EMBO J.*, **14**, 5646–5659.
Hurlin,P.J., Quéva,C. and Eisenman,R.N. (1997) Mnt, a novel Max-interacting protein is coexpressed with Myc in proliferating cells and mediates repression at Myc binding sites. *Genes Dev.*, **11**, 44–58.
Jacks,T., Fazeli,A., Schmitt,E.M., Bronson,R.T., Goodell,M.A. and Weinberg,R.A. (1992) Effects of an *Rb* mutation in the mouse. *Nature*, **359**, 295–300.
Jacobsen,K.A., Prasad,V.S., Sidman,C.L. and Osmond,D.G. (1994) Apoptosis and macrophage-mediated deletion of precursor B cells in the bone marrow of *Eμ-myc* transgenic mice. *Blood*, **84**, 2784–2794.
Kelly,K., Cochran,B.H., Stiles,C.D. and Leder,P. (1982) Cell-specific regulation of the c-*myc* gene by lymphocyte mitogens and platelet-derived growth factor. *Cell*, **35**, 603–610.
Koskinen,P.J., Ayer,D.E and Eisenman,R.N. (1995) Repression of Myc–Ras cotransformation by Mad is mediated by multiple protein–protein interactions. *Cell Growth Differ.*, **6**, 623–629.
Kretzner,L., Blackwood,E.M. and Eisenman,R.N. (1992) Myc and Max proteins possess distinct transcriptional activities. *Nature*, **359**, 426–429.
Lachman,H.M. and Skoultchi,A.I. (1984) Expression of c-*myc* changes during differentiation of mouse erythroleukaemia cells. *Nature*, **310**, 592–594.
Laherty,C.D., Yang,W.-M., Sun,J.-M., Davie,J.R., Seto,E. and Eisenman,R.N. (1997) Histone deacetylases associated with the mSin3 corepressor mediate Mad transcriptional repression. *Cell*, **89**, 349–356.
Lahoz,E.G., Xu,L., Schreiber-Agus,N. and DePinho,R.A. (1994) Suppression of Myc, but not E1a, transformation activity by Max-associated proteins, Mad and Mxi1. *Proc. Natl Acad. Sci. USA*, **91**, 5503–5507.
Lane,M.E., Sauer,K., Wallace,K., Nung Jan,Y., Lehner,C.F. and Vaessin,H. (1996) Dacapo, a cyclin-dependent kinase inhibitor, stops cell proliferation during *Drosophila* development. *Cell*, **87**, 1225–1235.
Langdon,W.Y., Harris,A.W., Cory,S. and Adams,J.M. (1986) The c-*myc* oncogene perturbs B lymphocyte development in Eμ-*myc* transgenic mice. *Cell*, **47**, 11–18.
Larsson,L.-G., Pettersson,M., Öberg,F., Nilsson,K. and Lüscher,B. (1994) Expression of *mad*, *mxi1*, *max* and c-*myc* during induced differentiation of hematopoietic cells: opposite regulation of *mad* and c-*myc*. *Oncogene*, **9**, 1247–1252.
Lee,E.Y.-H.P, Chang,C.-Y., Hu,N., Wang,Y.-C.J., Lai,C.-C., Herrup,K., Lee,W.-H. and Bradley,A. (1992) Mice deficient for Rb are nonviable and show defects in neurogenesis and haematopoiesis. *Nature*, **359**, 288–294.
Lee,E.Y.-H.P., Hu,N., Yuan,S.-S.F., Cox,L.A, Bradley,A., Lee,W.-H. and Herrup,K. (1994) Dual roles of the retinoblastoma protein in cell cycle regulation and neuron differentiation. *Genes Dev.*, **8**, 2008–2021.
Leonard,M.W., Lim,K.-C. and Engel,J.D. (1993) Expression of the chicken GATA factor family during early erythroid development and differentiation. *Development*, **119**, 519–531.
Liu,F., Wu,H.-Y., Wesselschmidt,R., Kornaga,T. and Link,D.C. (1996) Impaired production and increased apoptosis of neutrophils in granulocyte colony-stimulating factor receptor-deficient mice. *Immunity*, **5**, 491–501.
Lowell,C.A. and Soriano,P. (1996) Knockouts of Src-family kinases: stiff bones, wimpy T cells, and bad memories. *Genes Dev.*, **10**, 1845–1857.
Lymboussaki,A., Kaipainen,A., Hatva,E., Västrik,I., Jeskanen,L., Jalkanen,M., Werner,S., Stenbäck,F. and Alitalo,R. (1996) Expression of Mad, an antagonist of Myc oncoprotein function, in differentiating keratinocytes during tumorigenesis of the skin. *Br. J. Cancer*, **73**, 1347–1355.
Lyons,A.B. and Parish,C.R. (1994) Determination of lymphocyte division by flow cytometry. *J. Immunol. Methods*, **171**, 131–137.
Macleod,K.F., Hu,Y. and Jacks,T. (1996) Loss of *Rb* activates both *p53*-dependent and independent cell death pathways in the developing mouse nervous system. *EMBO J.*, **15**, 6178–6188.
Marcu,K.B., Bossone,S.A. and Patel,A.J. (1992) *myc* function and regulation. *Annu. Rev. Biochem.*, **61**, 809–860.
McKenna,S.L. and Cotter,T.G. (1997) Functional aspects of apoptosis in hematopoiesis and consequences of failure. *Adv. Cancer Res.*, **71**, 121–164.
Meroni,G. *et al*. (1997) Rox, a novel bHLHZip protein expressed in quiescent cells that heterodimerizes with Max, binds a non-canonical E box and acts as a transcriptional repressor. *EMBO J.*, **16**, 2892–2906.
Metcalf,D. (1984) *The Hemopoietic Colony Stimulating Factors*. Elsevier, Amsterdam.
Metcalf,D., Lindeman,G.J. and Nicola,N.A. (1995) Analysis of hematopoiesis in *max* 41 transgenic mice that exhibit sustained elevations of blood granulocytes and monocytes. *Blood*, **85**, 2364–2370.
Missero,C., Di Cunto,F., Kiyokawa,H., Koff,A. and Dotto,G.P. (1996) The absence of $p21^{Cip1/WAF1}$ alters keratinocyte growth and differentiation and promotes *ras*-tumor progression. *Genes Dev.*, **10**, 3065–3075.
Molkentin,J.D. and Olson,E.N. (1996) Defining the regulatory networks for muscle development. *Curr. Opin. Genet. Dev.*, **6**, 445–453.
Morgenbesser,S.D. and DePinho,R.A. (1994) Use of transgenic mice to study *myc* family gene function in normal mammalian development and in cancer. *Semin. Cancer Biol.*, **5**, 21–36.
Morgenbesser,S.D., Williams,B.O., Jacks,T. and DePinho,R.A. (1994) *p53*-dependent apoptosis produced by *Rb*-deficiency in the developing mouse lens. *Nature*, **371**, 72–74.
Morrison,S.J., Shah,N.M and Anderson,D.J. (1997) Regulatory mechanisms in stem cell biology. *Cell*, **88**, 287–298.
Poluha,W., Poluha,D.K., Chang,B., Crosbie,N.E., Schonhoff,C.M., Kilpatrick,D.L and Ross,A.H. (1996) The cyclin-dependent kinase

inhibitor $p21^{WAF1}$ is required for survival of differentiating neuroblastoma cells. *Mol. Cell. Biol.*, **16**, 1335–1341.
Prendergast,G.C., Lawe,D. and Ziff,E.B. (1991) Association of Myn, the murine homolog of Max, with c-Myc stimulates methylation-sensitive DNA binding and Ras cotransformation. *Cell*, **65**, 395–407.
Quéva,C., Hurlin,P.J., Foley,K.P. and Eisenman,R.N. (1998) Sequential expression of the MAD family of transcriptional repressors during differentiation and development. *Oncogene*, in press.
Raff,M.C. (1992) Social controls on cell survival and cell death. *Nature*, **356**, 397–400.
Raff,M.C. (1996) Size control: the regulation of cell numbers in animal development. *Cell*, **86**, 173–175.
Rao,G. *et al*. (1996) Mouse Sin3A interacts with and can functionally substitute for the amino-terminal repression domain of the Myc antagonist Mxi1. *Oncogene*, **12**, 1165–1172.
Roussel,M.F., Ashmun,R.A., Sherr,C.J., Eisenman,R.N. and Ayer,D.E. (1996) Inhibition of cell proliferation by the Mad1 transcriptional repressor. *Mol. Cell. Biol.*, **16**, 2796–2801.
Sawyers,C.L., Denny,C.T. and Witte,O.N. (1991) Leukemia and the disruption of normal hematopoiesis. *Cell*, **64**, 337–350.
Schneider,J.W., Gu,W., Zhu,L., Mahdavi,V. and Nadal-Ginard,B. (1994) Reversal of terminal differentiation mediated by p107 in $Rb^{-/-}$ muscle cells. *Science*, **264**, 1467–1471.
Schreiber-Agus,N., Chin,L., Chen,K., Torres,R., Rao,G., Guida,P., Skoultchi,A.I. and DePinho,R.A. (1995) An amino-terminal domain of Mxi1 mediates anti-Myc oncogenic activity and interacts with a homolog of the yeast transcriptional repressor SIN3. *Cell*, **80**, 777–786.
Sommer,A., Hilfenhaus,S., Menkel,A., Kremmer,E., Seiser,C., Loidl,P. and Lüscher,B. (1997) Cell growth inhibition by the Mad/Max complex through recruitment of histone deacetylase activity. *Curr. Biol.*, **7**, 357–365.
Soriano,P., Montgomery,C., Geske,R. and Bradley,A. (1991) Targeted disruption of the c-*src* proto-oncogene leads to osteopetrosis in mice. *Cell*, **64**, 693–702.
Stanton,B.R., Perkins,A.S., Tessarollo,L., Sassoon,D.A. and Parada,L.F. (1992) Loss of N-*myc* function results in embryonic lethality and failure of the epithelial component of the embryo to develop. *Genes Dev.*, **6**, 2235–2247.
Tsai,S. and Collins,S.J. (1993) A dominant negative retinoic acid receptor blocks neutrophil differentiation at the promyelocyte stage. *Proc. Natl Acad. Sci. USA*, **90**, 7153–7157.
Västrik,I., Kaipainen,A., Penttilä,T.-L., Lymboussakis,A., Alitalo,R., Parvinen,M. and Alitalo,K. (1995) Expression of the *mad* gene during cell differentiation *in vivo* and its inhibition of cell growth *in vitro*. *J. Cell Biol.*, **128**, 1197–1208.
Wang,J. and Walsh,K. (1996) Resistance to apoptosis conferred by Cdk inhibitors during myocyte differentiation. *Science*, **273**, 359–361.
Westin,E.H. *et al*. (1982) Expression of cellular homologues of retroviral *onc* genes in human hematopoietic cells. *Proc. Natl Acad. Sci. USA*, **79**, 2490–2494.
Yan,Y., Frisén,J., Lee,M.-H., Massagué,J. and Barbacid,M. (1997) Ablation of the CDK inhibitor $p57^{Kip2}$ results in increased apoptosis and delayed differentiation during mouse development. *Genes Dev.*, **11**, 973–983.
Zacksenhaus,E., Jiang,Z., Chung,D., Marth,J.D., Phillips,R.A. and Gallie,B.L. (1996) pRb controls proliferation, differentiation, and death of skeletal muscle cells and other lineages during embryogenesis. *Genes Dev.*, **10**, 3051–3064.
Zervos,A.S., Gyuris,J. and Brent,R. (1993) Mxi1, a protein that specifically interacts with Max to bind Myc–Max recognition sites. *Cell*, **72**, 223–232.
Zhang,P. *et al*. (1997) Altered cell differentiation and proliferation in mice lacking $p57^{KIP2}$ indicates a role in Beckwith–Wiedeman syndrome. *Nature*, **387**, 151–158.
Zhuang,Y., Cheng,P. and Weintraub,H. (1996) B-lymphocyte development is regulated by the combined dosage of three basic helix–loop–helix genes, *E2A*, *E2-2*, and *HEB*. *Mol. Cell. Biol.*, **16**, 2898–2905.

Received October 20, 1997; revised November 14, 1997; accepted November 17, 1997